Energies **2015**, *8*, 9344-9364; doi:10.3390/en8099344

OPEN ACCESS

energies

ISSN 1996-1073

www.mdpi.com/journal/energies

Article

Experimental Evaluation of Simple Thermal Storage Control Strategies in Low-Energy Solar Houses to Reduce Electricity Consumption during Grid On-Peak Periods

Kyoung-Ho Lee *, Moon-Chang Joo and Nam-Choon Baek

Solar Thermal Laboratory, New and Renewable Energy Research Division,
Korea Institute of Energy Research, Daejeon 305-343, Korea;
E-Mails: mcjoo@kier.re.kr (M.-C.J.); baek@kier.re.kr (N.-C.B.)

***** Author to whom correspondence should be addressed; E-Mail: khlee@kier.re.kr;
Tel.: +82-42-860-3525; Fax: +82-42-860-3538.

Academic Editor: Chi-Ming Lai

Received: 29 June 2015 / Accepted: 19 August 2015 / Published: 31 August 2015

Abstract: There is growing interest in zero-energy and low-energy buildings, which have a net energy consumption (on an annual basis) of almost zero. Because they can generate both electricity and thermal energy through the use of solar photovoltaic (PV) and solar thermal collectors, and with the help of reduced building thermal demand, low-energy buildings can not only make a significant contribution to energy conservation on an annual basis, but also reduce energy consumption and peak demand. This study focused on electricity consumption during the on-peak period in a low-energy residential solar building and considers the use of a building's thermal mass and thermal storage to reduce electricity consumption in summer and winter by modulation of temperature setpoints for heat pump and indoor thermostats in summer and additional use of a solar heating loop in winter. Experiments were performed at a low-energy solar demonstration house that has solar collectors, hot water storage, a ground-coupled heat pump, and a thermal storage tank. It was assumed that the on-peak periods were from 2 pm to 5 pm on hot summer days and from 5 pm to 8 pm on cold winter days. To evaluate the potential for utilizing the building's thermal storage capacity in space cooling and heating, the use of simple control strategies on three test days in summer and two test days in the early spring were compared in terms of net electricity consumption and peak demand, which also considered the electricity generation from solar PV modules on the roof of the house.

Keywords: peak demand; setpoint control; peak period; low-energy solar house; building thermal mass; buffer thermal storage

1. Introduction

Recently, a number of studies have been conducted on reducing electricity demand on the national power grid during peak periods. There is also a growing interest in zero- or low-energy solar houses that consume nearly zero net energy annually. Zero- and low-energy solar houses exploit not only renewable energy technologies such as solar photovoltaic (PV) systems to convert solar energy, but also building efficiency technologies to achieve the goal of near-zero energy consumption. Solar houses can generate both electricity and thermal energy using solar PV modules and solar thermal collectors. A heat pump system can be installed to meet space cooling demand and part of the space heating demand. With the help of building energy efficiency technologies such as better insulation and high-performance windows, the thermal demand of low-energy houses can be reduced to less than half that of conventional houses. Thus, low energy houses can significantly reduce not only annual energy consumption but also energy consumption during the peak demand period. Many low-energy houses have heating and cooling systems with both thermal storage for solar thermal collectors and heat pumps. The thermal storage system can be used to shift the thermal loads from peak periods to off-peak periods. There are two thermal storage methods that are suitable for use in a building. One is to use building thermal mass and the other is to install a thermal storage system. In the case of residential buildings, the volume of a thermal storage tank cannot be very large; it can be used only as a buffer storage tank between the thermal load and the thermal energy supply system. However, even a small volume of buffer thermal storage could be used effectively for shifting the thermal load from peak to off-peak periods in low-energy houses because the thermal demands of low-energy houses are lower than those of conventional houses. A number of studies have been conducted to evaluate the combined use of building thermal mass and thermal storage system to reduce the peak thermal demand or energy consumption [1–7]. Sun *et al.* [1] reviewed and summarized the control method on peak load shifting control by using cold thermal energy storage. They focused on space cooling operation in commercial buildings. Ban *et al.* [2] investigated the potential of cool thermal energy storage in building sector. They evaluated the impact of cool thermal energy storage and its integration with renewable energy systems by using a simplified mathematical model and a software tool H2RES. Henze *et al*. [3] evaluated the optimal control of combined thermal storage with active and passive building thermal storage. They simulated an office building by using the TRNSYS simulation tool to evaluate the optimal control method for building space cooling. Liu *et al.* [4,5] developed a simulated reinforced learning control for active and passive building thermal storage and evaluated the method at a demonstration small office building for space cooling period. Thermal storage was composed of building thermal mass and ice thermal storage system. Hajiah and Krarti [6,7] also studied the optimal control of combined thermal storage by using ice storage and building thermal mass for space cooling in a simulated office building. In particular, for demand-limiting control, the efficient use of a thermal storage system can be achieved using non-linear setpoint modulation to obtain constant cooling demand during the on-peak period [8–10]. Lee and Braun [8] employed a gray-box building

demand model to determine an optimal setpoint trajectory for minimizing peak cooling demand in commercial buildings; this method is termed demand-limiting control. They [9,10] simplified the method to determine a near-optimal setpoint trajectory by developing data-driven method and semi-analytical method and showed that the simplified methods were considerably effective compared to the model-based optimal method. However, most studies focused on the combined use of building thermal mass and thermal storage for space cooling in office buildings.

Several studies have been conducted on low-energy houses having thermal storage, whereas, few have been conducted the integrated use of thermal storage in residential buildings to reduce energy consumption during the on-peak period. More studies are needed on the combined use of building thermal mass and thermal storage systems to maximize the ability to reduce peak demand or energy consumption during peak periods in residential buildings, particularly in low-energy buildings that have both solar energy and thermal energy storage systems installed for ensuring more effective energy use.

Recently, in particular in Korea, national peak electric demand occurs not only on summer days but also on winter days because of the electrification of building heating systems and heaters in the industrial sector. Formerly, studies pertaining to the use of thermal storage for load control mainly focused on the space cooling. Therefore, it is worthwhile to investigate measures for reducing electricity consumption during the on-peak period of both winter days and summer days.

This paper analyzes the use of building thermal mass and buffer thermal storage to reduce energy consumption during peak periods in electricity-based low-energy solar houses during both space cooling and heating operations. In particular, the study focuses on electricity-based solar houses that make use of solar water heating system and heat pump to supply hot water by using floor heating systems for space heating and chilled water with a fan-coil unit system for space cooling, respectively. Experiments were performed for a low-energy solar demonstration house with a heat pump system and buffer thermal storage by changing the setpoints for the buffer storage and the indoor space. In space heating mode, solar thermal energy was employed to use the collected solar thermal energy during the on-peak period. The peak period is assumed to be from 2 pm to 5 pm for the space-cooling period and 5 pm to 8 pm for the space-heating period. The performance of control strategies using buffer thermal storage only and combined use of building thermal mass and buffer thermal storage are evaluated in terms of electricity consumption and net energy consumption. The electricity used was generated by only a solar PV system installed on the roof of the house.

2. Description of Demonstration House

A house was built in 2009 to demonstrate the operation of a low-energy solar house [11]. The building is a reinforced concrete structure with two stories and one underground level—A building area of 107.0 m^2 and a total floor area of 152.0 m^2. The house includes a solar PV module on its roof and an array of solar collectors in its wall. High density, colored, reinforced fiber cement panels made up the outer walls. An architectural overview of the house is presented in a paper by Lee *et al.* [11]. The building is located in the city of Daejeon, a major city in Korea. The annual cooling and heating demands of the house were 23.2 kWh/m^2 for space cooling and 41.8 kWh/m^2 for space heating, according to annual monitoring during 2010 [12].

Solar collectors are installed vertically on the south-facing façade; solar PV modules are installed on the roof at a 30 ° angle. The area of the solar collectors is 25 m^2; the rated capacity of the solar PV modules is 3.15 kW. The volume of the solar hot water storage tank is 0.4 m^3. The volume of the buffer storage tank is 0.8 m^3. The cooling capacity of the ground-coupled heat pump is 3 kWth. Figure 1 shows the heating and cooling system, consisting of a solar heating system and a ground-source heat pump installed in the building's basement. The system was renovated to the current configuration in early 2011 from the original system configuration [12]. Figure 1 presents a heating and cooling mode of the system in Figure 1a,b respectively. For space cooling, the heat pump runs to maintain the chilled water at the middle of the buffer storage tank at a setpoint. The chilled water of the buffer storage tank is circulated to a fan coil unit (FCU) to supply cooled air indoors. The indoor space is conditioned by FCU units installed on the ceiling in each room. The FCU units are controlled via signals from thermostats. The heat pump is used for domestic hot water heating but also for space heating as a backup heater for the solar heating system. The heat pump operates based on the temperature inside the buffer storage tank. For space heating, the heat pump operates similarly to in space-cooling mode; it maintains the (warm) water at the middle of the buffer storage tank at a setpoint. The warm water of the tank is circulated to the floor piping system in each room to meet the space setpoint, which can be adjusted by the thermostats. Hot water is also produced by solar collectors. In the space-heating period, hot water is circulated to the buffer storage tank after the heat has been transferred to the solar hot water storage tank. This operation proceeds according to the temperature difference between the solar collector outlet and the lower part of the buffer storage tank.

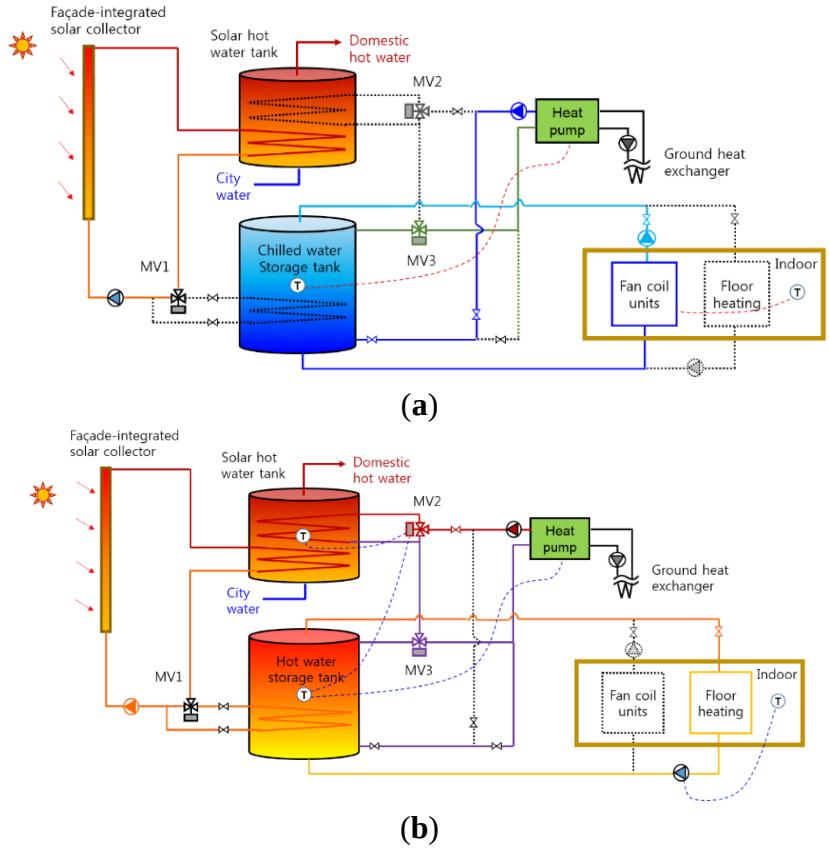

Figure 1. Schematic diagram for (**a**) cooling and (**b**) heating modes.

3. Setpoint Control Strategies Using Thermal Storage

The primary objective of this study is to evaluate simple control strategies to minimize electricity consumption for space cooling and heating during peak periods via load shifting. In this study, the electricity needed for space cooling and heating is consumed mainly by the heat pump. The other pieces of equipment used for space cooling and heating are the chilled/hot water circulation pumps and FCUs. Therefore, it is critical to minimize the use of the heat pump during the peak period, while maintaining a minimal sacrifice of thermal comfort during space cooling and space heating.

The control strategies applied in this study adjust the setpoint temperatures for the heat pump and the indoor space to utilize thermal storage to shift thermal demand during the on-peak period to the time period prior to the on-peak period. Two different control strategies were considered for space cooling operation: buffer storage control (BSC) and combined storage control (CSC). The BSC strategy uses cool thermal storage in a buffer storage tank. This method stores more cool thermal energy by subcooling the chilled water prior to the peak period by lowering the setpoint temperature of the heat pump, and then, increasing the setpoint temperature during the peak period to minimize heat pump use during that period. The setpoint temperature during the peak period should be at highest allowable level that can still be used for space cooling. The other potential method of using thermal storage is to use building thermal mass by precooling the indoor space prior to the peak period by lowering the setpoint temperature, which will result in less demand for energy for cooling during the peak period, because the shallow surface of the building structures is already precooled and heat is transferred from the indoor air to the cooled structure, which results in less cooling demand for the space. The setpoint temperatures should be in the range of thermal comfort temperatures. To maximize the impact of building thermal mass, the setpoint prior to the peak period can be set at the lowest comfortable temperature, and during the peak period, can be set at the highest comfortable temperature. The other control strategy in this study is combined storage control (CSC), which combines building thermal mass control and BSC. Figure 2 presents the control strategies for conventional control (CC) and thermal storage control when space cooling is being carried out.

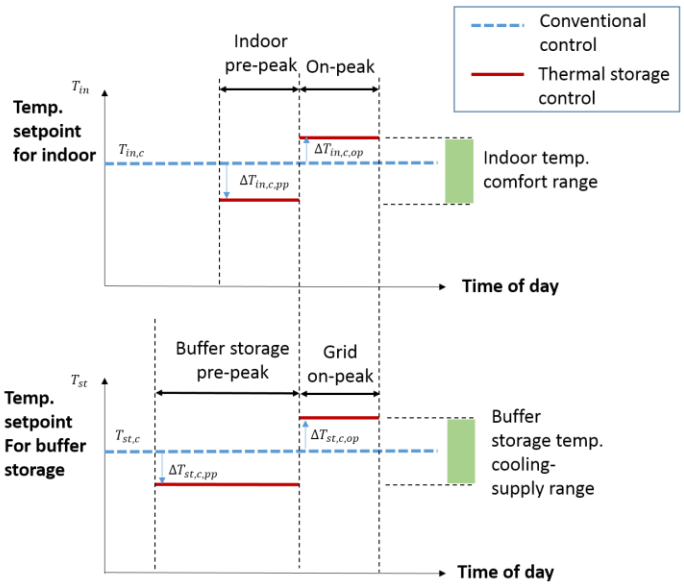

Figure 2. Schematic setpoint schedule for control strategies during cooling operation.

The dotted line indicates the setpoints for CC. The solid line indicates the setpoints for thermal storage control. The upper part of the figure shows the setpoint schedule for the indoor space; the lower part shows the buffer storage schedule. There are two thermal storage control strategies considered in this study: BSC and CSC. BSC needs a setpoint schedule only to minimize the impact on thermal comfort without changing the indoor setpoint temperature. CSC has setpoint schedules for both buffer storage and the indoor space to maximize the effect of thermal storage and reduce cooling energy demand and consumption. In actual applications, a site-specific thermal comfort temperature range and a buffer storage temperature range should be determined.

On a peak day in winter, a similar control strategy that uses buffer thermal storage and building thermal mass can be employed. In this study, the additional thermal storage of a solar hot water storage tank is involved. In addition to the temperature setpoint of the buffer hot water storage tank and the indoor space being adjusted before and during the on-peak period, hot water from the solar collectors is held in the solar hot water storage tank before the on-peak period using a motorized control valve MV1; then, hot water was circulated to the hot water storage tank using motorized control valves MV2 and MV3 during the on-peak period. This method also has a role in reducing the load on the heat pump and contributes to minimizing its use during the on-peak period. Figure 3 presents the control strategies for conventional and thermal storage controls during space heating. Compared to the strategy in space cooling seen in Figure 2, it is noted that additional setpoint schedules are involved regarding valves MV1, MV2 and MV3 to control solar heat storage. The valve control is based on differential temperature control. ΔT_{mv1} is defined as temperature difference between outlet temperature from the solar storage tank and temperature at lower part of the buffer storage tank and $\Delta T_{mv2,3}$ is expressed as temperature difference between temperature at the middle part of solar storage tank and temperature at middle part of buffer storage tank. Figure 4 shows the direction in which the thermal fluid flows with a thick solid line showing how MV1, MV2 and MV3 operate. Figure 4a presents thermal fluid flow prior to the on-peak period by controlling the thermal fluid flow bypassing the buffer storage tank to store solar heat in the solar storage tank. Figure 4b shows thermal fluid flow during the on-peak period to discharge the solar heat store in the solar storage tank into the buffer storage tank, increasing the temperature in the buffer storage tank. This reduces the chances of the heat pump working, considering that heat pump operation depends on the temperature of the buffer storage tank.

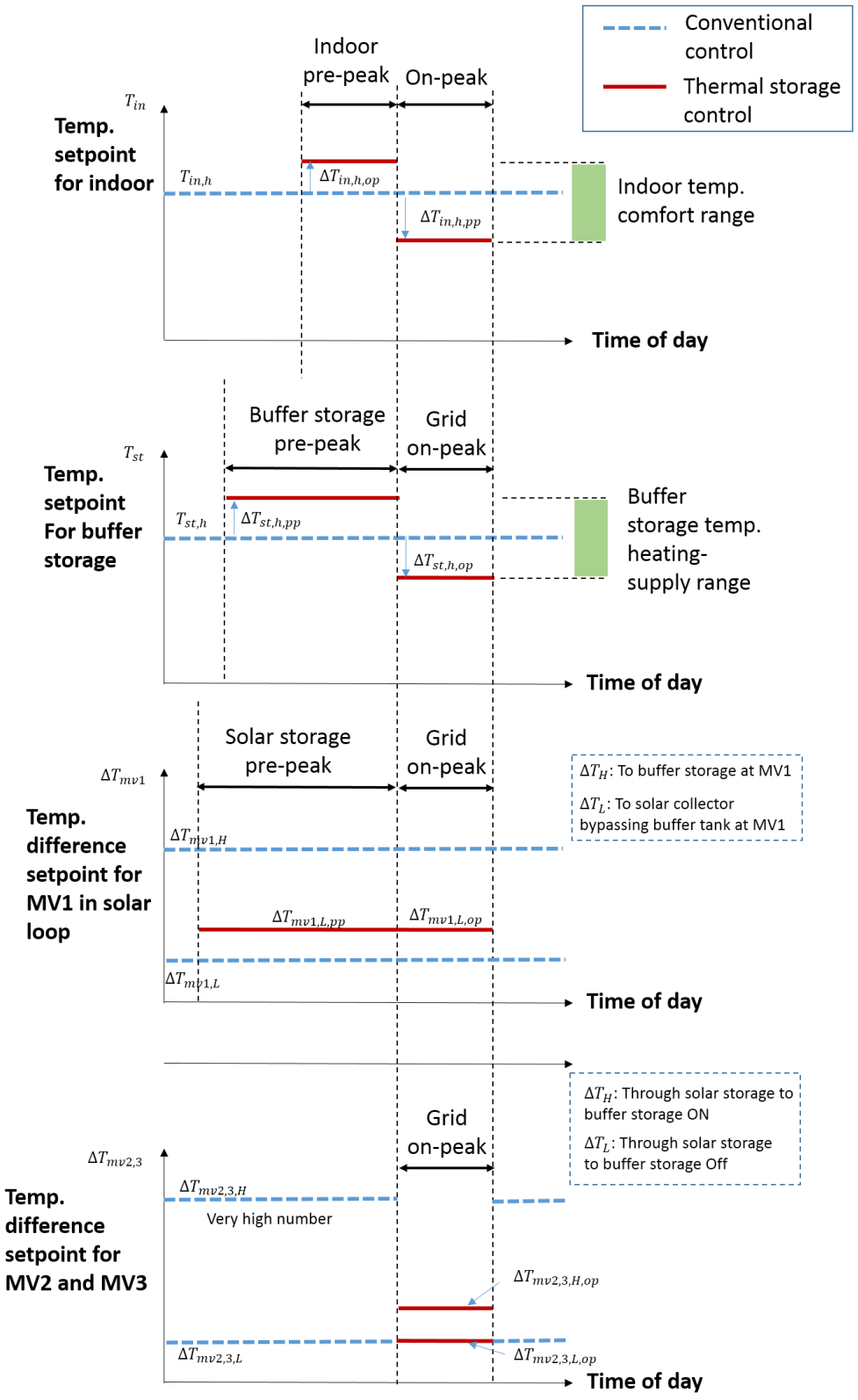

Figure 3. Schematic setpoint schedule for control strategies during heating operation.

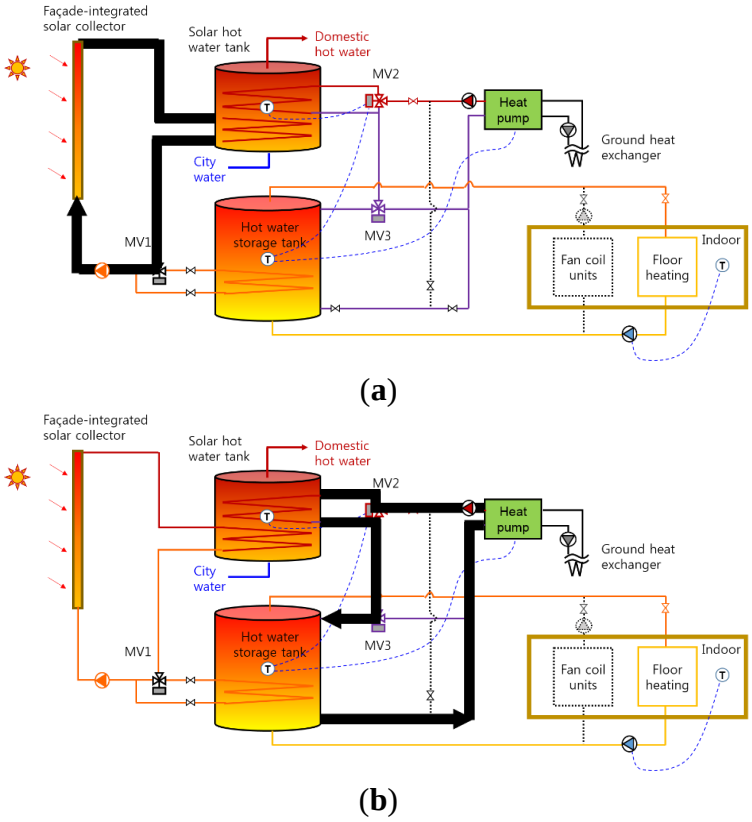

Figure 4. Flow diagram of solar storage control for (**a**) solar heat storage in solar storage tank with MV1 prior to on-peak period and (**b**) discharge from solar storage to buffer storage with MV2 and MV3 during on-peak period.

Table 1 compares the strategies for controlling thermal storage and the building's thermal mass that were used in this study. In the table, $T_{in,c}$ is the indoor cooling temperature setpoint used in the conventional control strategy, $\Delta T_{in,c}$ is the increment of the inside cooling temperature setpoint during the on-peak period, $T_{in,h}$ is the indoor heating temperature setpoint used in the conventional control strategy, $\Delta T_{in,h}$ is the increment of the indoor heating temperature setpoint during the on-peak period, $T_{st,c}$ is the heat pump cooling temperature setpoint inside the storage tank used in the conventional control strategy, $\Delta T_{st,c}$ is the increment of the heat pump cooling temperature setpoint during the on-peak period, $T_{st,h}$ is the heat pump temperature setpoint inside the storage tank used in the conventional control strategy, and $\Delta T_{st,h}$ is the increment of the heat pump heating temperature setpoint during the on-peak period.

Table 1. Strategies used to control temperature setpoints for thermal storage during space cooling and heating.

Mode	Time	Indoor				Chilled/Hot water storage tank			
		Before	**Pre-peak**	**On-peak**	**After**	**Before**	**Pre-peak**	**On-peak**	**After**
Space cooling	CC	$T_{in,c}$	$T_{in,c}$	$T_{in,c}$	$T_{in,c}$	$T_{st,c}$	$T_{st,c}$	$T_{st,c}$	$T_{st,c}$
	BSC	$T_{in,c}$	$T_{in,c}$	$T_{in,c}$	$T_{in,c}$	$T_{st,c}$	$T_{st,c} - \Delta T_{st,c,pp}$	$T_{st,c} + \Delta T_{st,c,op}$	$T_{st,c}$
	CSC	$T_{in,c}$	$T_{in,c} - \Delta T_{in,c,pp}$	$T_{in,c} + \Delta T_{in,c,op}$	$T_{in,c}$	$T_{st,c}$	$T_{st,c} - \Delta T_{st,c,pp}$	$T_{st,c} + \Delta T_{st,c,op}$	$T_{st,c}$
Space heating	CC	$T_{in,c}$	$T_{in,h}$	$T_{in,h}$	$T_{in,h}$	$T_{st,h}$	$T_{st,h}$	$T_{st,h}$	$T_{st,h}$
	CSC	$T_{in,h}$	$T_{in} + \Delta T_{in,h,pp}$	$T_{in,h} - \Delta T_{in,h,op}$	$T_{in,h}$	$T_{st,h}$	$T_{st,h} + \Delta T_{st,h,pp,h}$	$T_{st,h} - \Delta T_{st,h,op}$	$T_{st,h}$

Table 2 shows the action of the control valves MV1, MV2, and MV3 and setpoints associated with the operation of the control valves during on-peak periods. "Normal" in the table indicates normal operation status. The flow of heat-transfer fluid leaving the solar collector is controlled such that it bypasses the buffer hot water storage tank before the on-peak period; in this way, it increases the water temperature in the solar hot water storage tank such that it is higher than that in conventional operation. The valves MV2 and MV3 are operated so as to allow the circulating fluid to flow through both the solar hot water tank and the buffer hot water storage tank at the beginning of the on-peak period. This indicates discharge of stored heat from the solar hot water tank to the buffer hot water storage tank, and therefore, results in an increase in the water temperature in the buffer hot water storage tank at the onset of the on-peak period. The use of the solar hot water tank contributes to delaying the onset of heat pump operation during the on-peak period.

Table 2. Control modes applied to utilize solar heat during space heating.

	MV1			**MV2, MV3**		
	Before	**On-peak**	**After**	**Before**	**On-peak**	**After**
Flow	Bypass buffer tank	Bypass buffer tank	Normal	Normal	Through solar and buffer tanks	Normal
Set-points	$\Delta T_{mv1,H}$ $\Delta T_{mv1,L,pp}$,	$\Delta T_{mv1,H}$ $\Delta T_{mv1,L,op}$	$\Delta T_{mv1,H}$ $\Delta T_{mv1,L}$	Very high $\Delta T_{mv2,3,L}$	$\Delta T_{mv2,3,H,op}$ $\Delta T_{mv2,3,L}$	Very high $\Delta T_{mv2,3,L}$

4. Experimental Demonstration of Thermal Storage Control

4.1. Method of Experiment

Experimental tests were conducted in August and March at the demonstration house for space cooling and heating modes to evaluate the effectiveness of the thermal storage control methods. Because, in the demonstration house, there was no occupant during the test, two electric heaters were placed in the living room and near the kitchen space of the first floor to simulate the internal heat gains of residential buildings. The heater in the living room was scheduled to turn on each hour for 15 min at a 1 kW electric input to generate roughly 250 Wh of internal heat gain per hour [13]. The heater was operated from 6 am to 7 pm. Another electric heater was placed near the kitchen to simulate the internal heat gain from cooking by turning on the heater for 30 min at 7 am, 11 pm, and 5 pm. The electric heaters were not used for heating operation mode tests. Figure 5 shows the electric heaters used for cooling-mode tests.

Figure 5. Two electric heaters on the first floor inside the demonstration house to simulate internal heat gains.

The adjustments of the setpoints for the indoor space are performed by changing the setpoints of the thermostats in each room. The setpoint for buffer thermal storage is changed on the control display panel of the heat pump. All adjustments were performed manually. For the cooling test in the conventional control, $T_{in,c}$ was 26 ℃ and $T_{st,c}$ was 12 ℃, with an upper deadband of 3 ℃ for the whole day. For thermal storage control, $\Delta T_{in,c}$ was 2 ℃, $\Delta T_{pp,c}$ was 2 ℃ with an upper deadband of 1 ℃, and $\Delta T_{op,c}$ was 8 ℃ with an upper deadband of 1 ℃. For the heating test, in the conventional control, $T_{in,h}$ was 28 ℃ and $T_{st,h}$ was 45 ℃ with an upper deadband of 2 ℃ for the whole day. For thermal storage control, $\Delta T_{in,h}$ was 2 ℃, $\Delta T_{pp,h}$ was 0 ℃ with an upper deadband of 1 ℃, and $\Delta T_{op,h}$ was 8 ℃ with an upper deadband of 2 ℃. It should be noted that the indoor heating temperature setpoint was set higher than the normal temperature setpoint of 21 to 23 ℃ because the heating test was conducted on days that were not so cold in March. In conventional control of motor valve MV1, $\Delta T_{mv1,H}$ and $\Delta T_{mv1,L}$ were set to 12 ℃ and 3 ℃, respectively, and $\Delta T_{mv1,L,pp}$ and $\Delta T_{mv1,L,op}$ were increased to 15 ℃ in order to bypass the buffer storage tank when solar heat is collected. For conventional control of motor valves MV2 and MV3, $\Delta T_{mv23,H}$ and $\Delta T_{mv23,L}$ were set to 50 ℃ which is very high value and 3 ℃, respectively; $\Delta T_{mv23,H,op}$ was set to 10 ℃.

The chilled water pump for space cooling was always on during the test to investigate the temperature variation of the chilled water in the buffer storage tank. However, the electric power consumption of the chilled water pump is assumed to be synchronized to the operation status of the FCU, which is a reasonable approach when simulating the actual situation.

The measurement and data acquisition system logs solar radiation, outdoor temperature, indoor temperatures, and water temperature in the buffer storage tank; inlet and outlet flow temperatures of the heat pump; inlet and outlet temperatures of the buffer storage tank; power consumption of the FCU, heat pump, and its associated components; power generated by the solar PV system; and flow rate of the chilled water from the heat pump, which is used for space cooling. All data was recorded using a data logger and a computer at a time interval of 1 min. The water temperature was measured using a four-wire RTD (resistance temperature detector) sensor; the indoor air temperatures were measured using calibrated thermocouple sensors. The flow rates of the chilled water from the heat pump and from the buffer storage tank were measured once using an electro-magnetic flow meter; thereafter, it was assumed that the flow rate was constant. The operation status of each pump was recorded to estimate the electricity consumption. The measuring points for the indoor temperatures in each room were located two meters above the floor; however, this seems quite high to evaluate the indoor thermal environment. Therefore, the measured indoor temperature data were modified based on the temperature difference from the temperature measured near the thermostat using a well-calibrated temperature sensor.

4.2. Experimental Results

Experiments were performed in August and March for space-cooling and space-heating mode tests, respectively. After the tests, three test days with similar weather conditions were selected from the cooling-mode test days to compare the energy saving performance of the three different control strategies, *i.e.*, BSC and CSC with CC. Similarly, two test days with similar weather conditions were selected for the heating-mode test to evaluate the two control strategies, *i.e.*, CC and CSC.

To evaluate the impact on the electricity consumption of the house, the energy consumption of the air-conditioning system was measured; however the electricity consumption of the house for lighting and plug loads was approximated, as seen in Figure 6 [14]. This profile was obtained based on electricity consumption data measured in six apartments in high-rise residential building complexes [14].

Figures 7 and 8 compare the outdoor temperature and the horizontal solar radiation for the three selected days for space-cooling mode tests and two selected days for space-heating mode tests. Regarding the similarity of the weather conditions between the compared test days, the root-mean squared differences for the three days are below 10% and 3% for solar radiation and ambient temperature, respectively. In fact, we found that the highest national grid peak demand in August of 2013 happened on the day in which the BSC strategy was tested. The peak demand was 7401.5 MW with a 6.4% reserve margin rate [15]. The day of the week was Monday. On the CSC test day, the national grid had a similar peak demand of 7321.6 MW. The peak demand on the test day with CC was much lower, at 6271.0 MWh, because it was a Sunday. The test days for space-heating mode occurred in March; therefore, national grid peak demand did not occur during the test days.

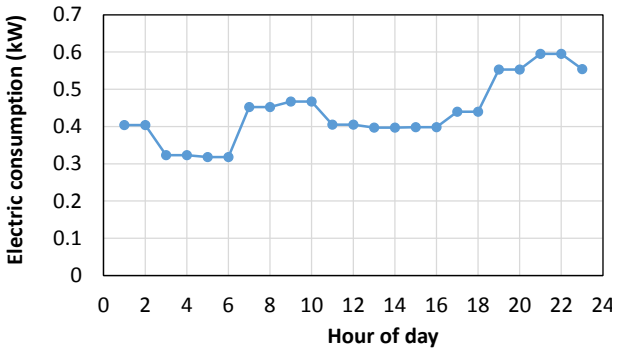

Figure 6. Approximated electricity load profile of other usage for one day (comprising lighting and plug load).

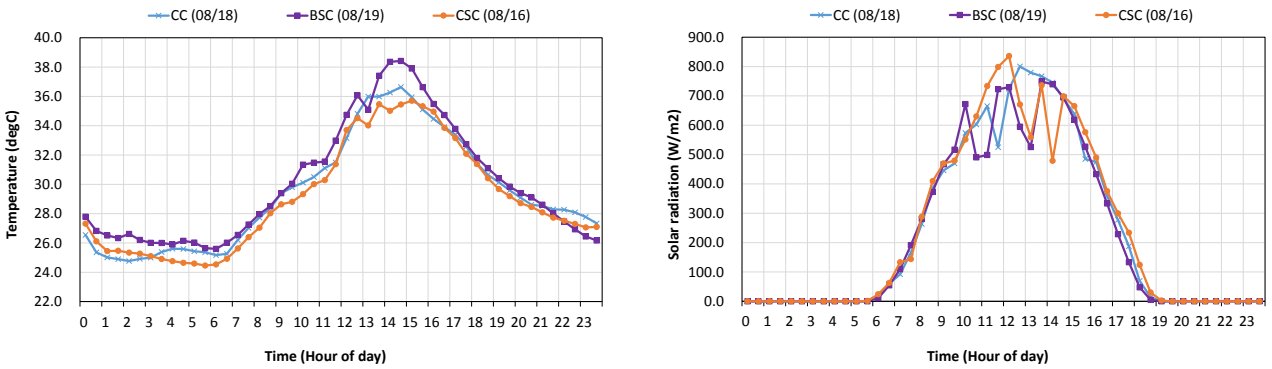

Figure 7. Comparison of weather conditions, (**a**) outdoor temperature and (**b**) global horizontal solar radiation, for three space-cooling operation test days with CC, BSC, and CSC.

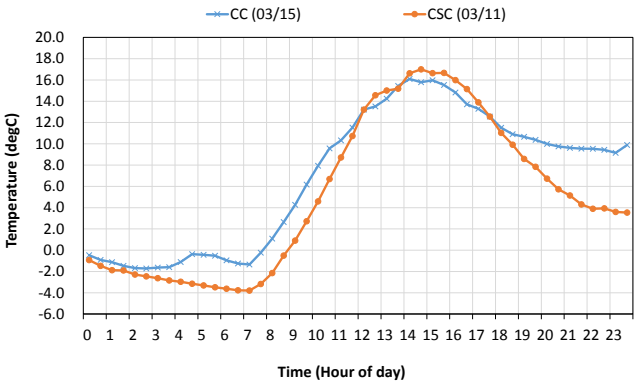

(**a**)

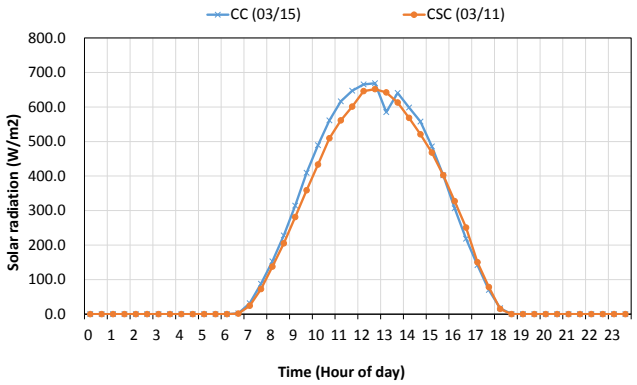

(**b**)

Figure 8. Comparison of weather conditions, (**a**) outdoor temperature and (**b**) global horizontal solar radiation, for two space-heating operation test days with CC and CSC.

Figure 9 represents the net electricity consumption of the three different control strategies for cooling-mode tests with average values for 30-min intervals. Table 3 presents electricity consumption during the peak period for the three control strategies. Table 4 compares similar results regarding electricity consumption for the whole test day. "FCU & Pchw" indicates electricity consumption of the FCU and the chilled water circulation pump. "Heat pump and pumps" indicates the electricity consumption of the heat pump, the fluid circulation pump between the heat pump and the ground heat exchanger, and the fluid circulation pump between the heat pump and the buffer storage. The electricity generation from the solar PV system is negative in the figures so that the net electricity consumption can be negative if the PV generation exceeds the total electricity consumption.

As shown in Figure 9a, the net electric power consumption with CC during the peak period from 2 pm to 5 pm was negative for 1 h, from 2 pm to 3 pm, and became positive for the remaining 2 h, from 3 pm to 5 pm. Due to the nearly cyclic power demand of the heat pump system, the power demand alternates with a period of 3–4 h. The net electricity consumption during the peak period is 1.77 kWh, with a total electricity consumption of 6.15 kWh and a solar power generation of 4.38 kWh. The net energy consumption with BSC, as seen in Figure 9b, maintains a negative value except during the last 30 min, at 0.15 kW, from 4:30 pm to 5 pm during the peak period. Because of the subcooling of the buffer storage prior to the peak period, the electricity consumption of the heat pump increased much more than that with CC from 9 am to 2 pm. The heat pump did not run during the peak period; however, the FCU was running throughout the peak period. It was observed that the FCU power consumption

increased gradually during the peak period. The temperature in the buffer storage tank increased slowly in the range between the lower setpoint and the higher setpoint because the setpoint for the buffer storage tank was set to 20 °C at 2 pm, from 10 °C at 9 am. As the temperature of the chilled water in the buffer storage tank rises, the FCU in each room requires more cool air supply to meet the indoor setpoint, resulting in a longer FCU operation time. The net energy consumption during the peak period with BSC, seen in Table 3, is negative, at −1.90 kWh, with a total electricity consumption of 2.41 kWh and a solar power generation of 4.30 kWh. As seen in Figure 9b, the net power demand during the peak period had its lowest value at the onset time of the peak, *i.e.*, at 2 pm; then it gradually increased toward the end of the peak period. It was observed that the shape of the net power demand curve is affected by the shape of the generated power curve, because the electricity demand of the house is significantly reduced in BSC while the power generated by the solar PV system is high. For CSC, the net energy consumption seen in Figure 9c is negative throughout the peak period. Because of the subcooling and precooling requirements prior to the peak period, the electricity use of the heat pump increased much more than with CC or BSC. However, it should be noted that neither the heat pump nor the FCU ran during the peak period. Because the building thermal mass was cooled by precooling before the peak period, the cooling demand of the FCU and buffer storage during the peak period was reduced to zero in this case. This means that the indoor space temperature stayed below the setpoint (28 °C) until the end of the peak period, otherwise the FCU would have turned on during the peak period. The net energy consumption with CSC during the peak period presented in Table 3 is −2.92 kWh, with a total energy consumption of 1.19 kWh and a solar power generation of 4.15 kWh. This means that the electricity production from the house exceeded the electricity consumption of the house, and therefore, it supplied excess electricity to the grid during the peak period. It should also be noted that the operating time of the heat pump increased by 2 and 4 h after the peak period with CSC and BSC, respectively, compared to CC. The reason that the operating time of the heat pump after the peak period with BSC is longer than that with CSC is that the water temperature is higher in the buffer storage tank in BSC. The increased thermal load due to precooling of the building thermal mass is transferred to the buffer storage tank before the peak period, resulting in higher energy consumption by the heat pump in CSC than in BSC. This phenomenon reduced the operating time of the heat pump after the peak period in CSC. The energy consumption of the cooling system for the whole day, presented in Table 4, is roughly 23.3 to 23.5 kWh, which is not significantly different for different control strategies. This result, however, proves that the thermal storage control of the buffer storage and the building thermal mass does significantly reduce the cooling energy consumption during the peak period without sacrificing electricity consumption for the whole day. Figure 10 shows temperatures in the solar hot water tank and the buffer storage tank, and the heat pump electric power in BSC and CSC. The temperature in the buffer storage decreases from 9 am to 11 am, and then, increases until 2 pm, because the indoor setpoints were adjusted to a lower comfort limit temperature for precooling. During the on-peak period, the temperature increases more rapidly in the case of BSC, compared to CSC, both because there was no precooling in BSC control and because some of the FCU units should run when the indoor temperature reaches the indoor setpoint during on-peak period, which does not happen in CSC control.

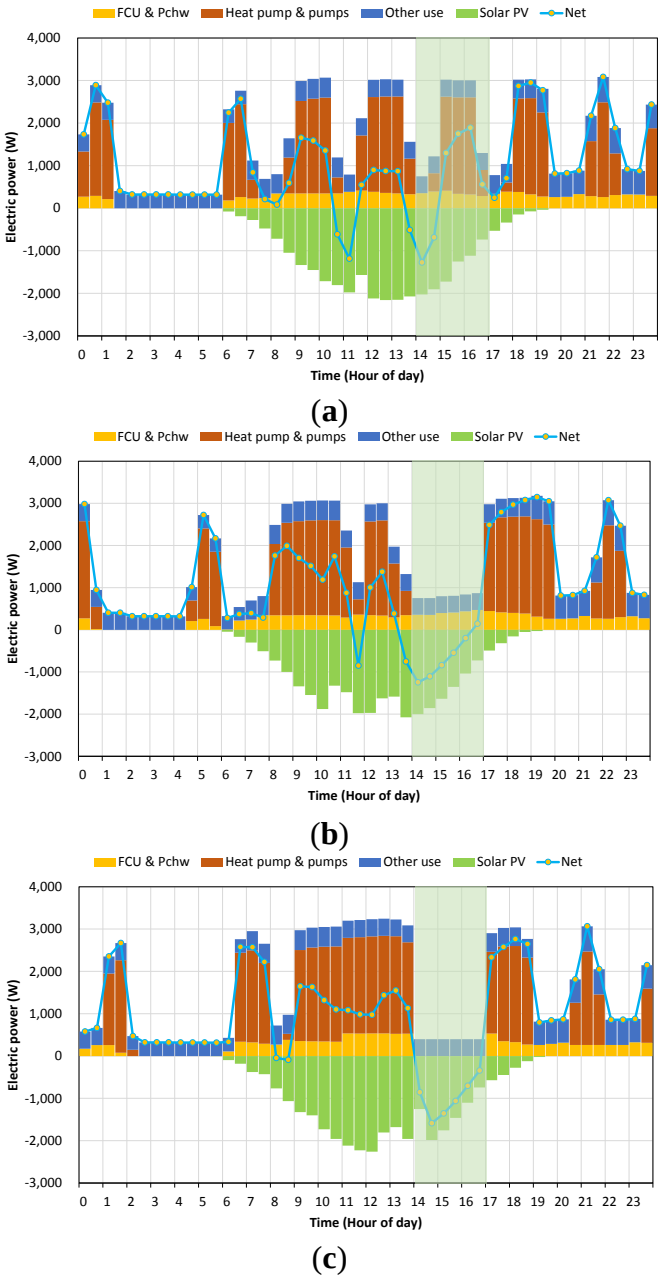

Figure 9. Energy consumption for different control strategies (**a**) CC; (**b**) BSC; and (**c**) CSC in space-cooling operation mode tests.

Table 3. Electricity consumption during on-peak period with three different control strategies for space-cooling-mode tests.

(Unit: kWh)	CC	BSC		CSC	
	Energy consumption	Energy consumption	Energy saving (%)	Energy consumption	Energy saving (%)
Heat pump and pumps	3.90	0.00	100.00	0.00	100.00
FCU and PCHW	1.05	1.21	−15.24	0.00	100.00
Cooling sum	4.95	1.21	75.56	0.00	100.00
Other use	1.19	1.19	0.00	1.19	0.00
Total sum	6.15	2.41	60.81	1.19	80.65
Solar PV	−4.38	−4.30	1.83	−4.15	5.25
Net sum	1.77	−1.90	207.34	−2.95	266.67

Table 4. Electricity consumption for the whole day for three different control strategies for space-cooling-mode tests.

(Unit: kWh)	CC	BSC		CSC	
	Energy consumption	Energy consumption	Energy saving (%)	Energy consumption	Energy saving (%)
Heat pump and pumps	23.44	23.30	0.60	23.49	−0.21
FCU and PCHW	6.23	6.32	−1.44	5.67	8.99
Cooling sum	29.66	29.62	0.13	29.16	1.69
Other use	10.38	10.38	0.00	10.38	0.00
Total sum	40.04	40.00	0.10	39.54	1.25
Solar PV	−15.60	−14.67	5.96	−15.68	−0.51
Net sum	24.44	25.33	−3.64	23.86	2.37

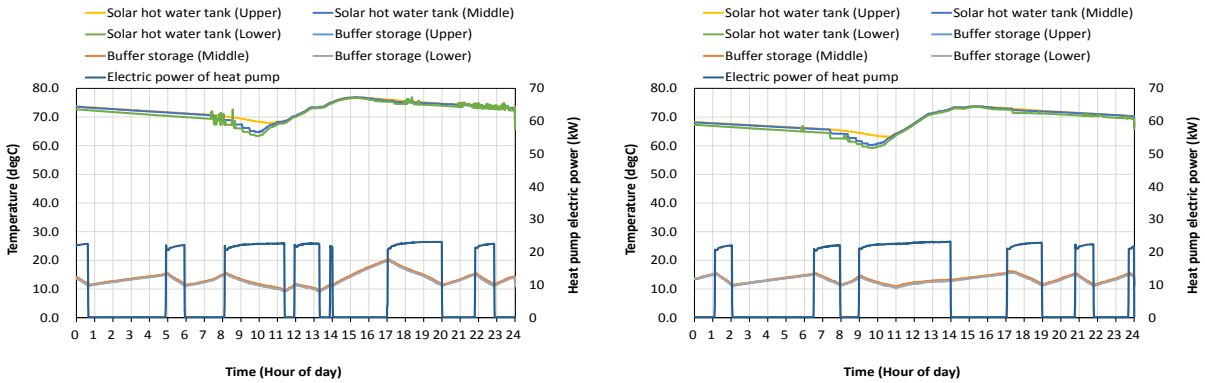

Figure 10. Temperature variation in solar hot water tank and buffer storage tank, and heat pump electric power for cooling operation mode test using (**a**) BSC and (**b**) CSC.

Figure 11 presents the net electricity consumption of the two different control strategies for the heating-mode test with average values at 30min intervals. As shown in Figure 11a, the net electric power consumption with CC during the peak period from 5 pm to 8 pm gradually increased, and the peak occurred around 7 pm. The net electricity consumption during the peak period was 3.84 kWh with a total electricity consumption of 4.04 kWh and a solar power generation of 0.20 kWh. The net energy consumption with CSC, as seen in Figure 11b, was maintained near zero during the peak period. Because of the heating requirements of the heat pump prior to the peak period, similar to in the cooling test, the electricity consumption of the heat pump for heating water in the buffer storage increased much more than that with CC. The heat pump did not heat water in the buffer storage during the on-peak period. Hot water from a solar storage tank was also supplied to the buffer storage at the beginning of the on-peak period so as to raise the temperature in the upper part of the buffer storage tank. This can provide another benefit, by reducing the likelihood of heat pump operation during the on-peak period. Figure 12 shows the water temperatures in the solar hot water tank and the buffer storage tank and the electric power of the heat pump in CSC in a space-heating-mode test. The temperature in solar hot water tank increases rapidly prior to the peak period; it maintains a temperature at the allowable high limit temperature, around 75 ℃, and then, reduces the temperature rapidly from the beginning of the on-peak period,

because the flow circulating between the solar hot water tank and the buffer storage tank was initiated to supply thermal energy stored in the solar hot water tank to the buffer storage tank, resulting in an increase in temperature in the upper part of the buffer storage tank. As seen in Figure 11b, the net power demand during the peak period falls to its lowest value at the onset time of the peak at 5 pm, and then, slowly rises until the end of the peak period. It was observed that the shape of the net power demand curve is not strongly affected by the shape of the generated power curve, because the electricity demand of the house is significantly reduced when using CSC, whereas the power generated by the solar PV system is negligible during the on-peak period. The net energy consumption with CSC during the peak period is 1.02 kWh, with a total energy consumption of 1.43 kWh and a solar power generation of 0.41 kWh.

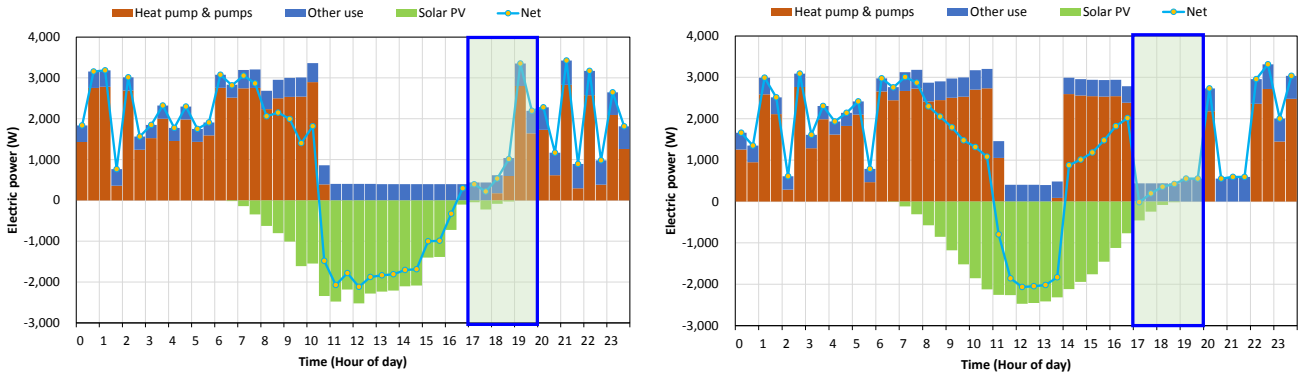

Figure 11. Electricity consumption for different control strategies (**a**) CC and (**b**) CSC in space-heating operation mode tests.

In order to evaluate the impact of building thermal mass of the house on thermal demands after the storage control test, the electric energy consumed by the heat pump was compared overnight for 7 h. The results obtained—13,259 Wh in conventional control and 13,488 Wh in thermal storage control—Did not show a significant difference between conventional control and thermal storage control.

Tables 5–7 summarize the electricity consumption and peak demand for the cooling and heating tests to compare the control strategies that use thermal storage to the conventional strategy. Negative energy savings means that the electricity consumption in thermal storage control is larger than that with conventional control. The net electricity consumption for the whole day showed quite different results for space-cooling and space-heating tests. The total energy consumption for the whole test day with BSC and CSC control for cooling mode was only marginally different from that observed for conventional control in the cooling test; however, it was roughly 12% higher in the heating test. However, compared to conventional control, the energy consumption during the on-peak period with CSC control was reduced by roughly 80% and 64% in the cooling and heating tests, respectively. Compared to conventional control, peak demand was also significantly reduced (86% and 83% in the cooling and heating test, respectively) when CSC control was adopted. If the impact of the solar PV electricity generation on the electricity consumption and peak demand of the building is considered in the cooling test, the energy savings are further increased. In the heating test, the solar radiation received during the on-peak period was not significant; therefore, the impact of the solar PV module was not as large as in

the cooling test. The on-peak period for the heating test was assumed to occur in the late afternoon. It should also be noted that the solar radiation received was not exactly the same on the two test days, and therefore, the solar electricity generated on each day was slightly different.

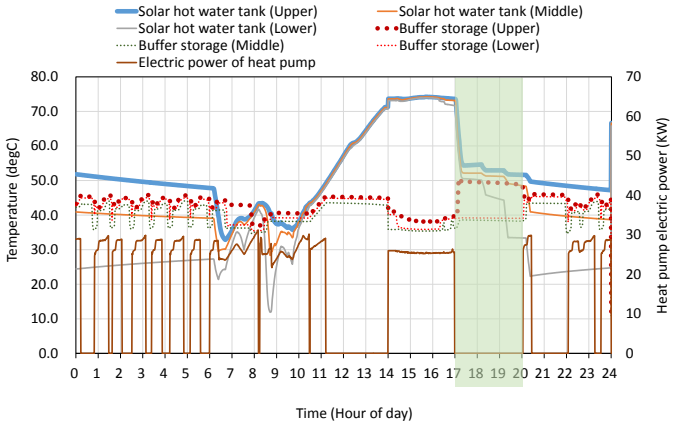

Figure 12. Temperature variation in solar hot water tank and buffer storage tank, and heat pump electric power for space-heating operation mode test with CSC.

Table 5. Comparison of electricity consumption and peak demand for two test days using conventional and peak reduction control strategies in space-cooling-mode tests(BSC in space cooling mode).

	Control strategy	CC	BSC	Saving (%)
Energy consumed during the day (kWh/day)	Without PV	40.04	40.00	0.10
	With PV	24.44	25.33	−3.64
Energy consumed during on-peak time (kWh/on-peak)	Without PV	6.15	2.41	60.81
	With PV	1.77	−1.90	207.34
Peak demand during on-peak time (kW/on-peak)	Without PV	3.02	0.87	71.19
	With PV	1.89	0.14	92.59

Table 6. Comparison of electricity consumption and peak demand for two test days using conventional and peak reduction control strategies in space-cooling-mode tests (CSC in space cooling mode).

	Control strategy	CC	CSC	Saving (%)
Energy consumed during the day (kWh/day)	Without PV	40.04	39.54	1.25
	With PV	24.44	23.86	2.37
Energy consumed during on-peak time (kWh/on-peak)	Without PV	6.15	1.19	80.65
	With PV	1.77	−2.95	266.67
Peak demand during on-peak time (kW/on-peak)	Without PV	3.02	0.40	86.75
	With PV	1.89	−0.34	117.99

Table 7. Comparison of electricity consumption and peak demand for two test days using conventional and peak reduction control strategies in space-heating-mode tests (CSC in space heating mode).

	Control strategy	CC	CSC	Saving (%)
Energy consumed during the day (kWh/day)	Without PV	41.44	46.68	−12.65
	With PV	26.17	30.33	−15.91
Energy consumed during on-peak time (kWh/on-peak)	Without PV	4.04	1.43	64.53
	With PV	3.84	1.02	73.36
Peak demand during on-peak time (kW/on-peak)	Without PV	3.35	0.55	83.51
	With PV	3.35	0.55	83.51

4.3. Limitations of the Study

This study compared several test days with different control strategies but with similar weather conditions for space-cooling and space-heating operations. The test results show the potential of simple control strategies to reduce the electricity consumption and peak electric demand during grid on-peak periods. Overall electricity consumption on the compared testing days showed results that were not significantly different. For a more exact comparison, one should perform evaluations using calibrated simulation tools and compare longer test days after the controls are applied. Nevertheless, the result that electricity consumption of the whole test days are not very different indicates that thermal storage control strategies can be applied under time-varying electric rate structures to benefit from lower electricity rates before and after the on-peak period.

In particular, heating operation tests were performed in March, meaning that weather conditions were not cold enough to match grid peak power days, and therefore, result in lower heating demand in the demonstration house. It should be noted that indoor setpoints were raised (resulting in higher heating demand) to simulate cold peak days. Therefore, the test results for heating operation do not provide an absolute comparison (but instead, a relative comparison) between thermal storage control and the conventional control strategy.

In this study, internal heat gain was simulated according to reference [13]. But it should be noted that different internal heat gains should be considered according to different geographical region and cooling appliances.

Climatic conditions could affect the impact of the thermal storage control because weather conditions such as ambient temperature, solar radiation, and humidity are major factors of thermal demands in buildings. The average climatic conditions of the test site [16] is summarized in Table 8.

Table 8. Monthly average climatic conditions of test site (Daejeon in Korea, Latitude 36.4 °N, 127.4 °E, Elevation of 72 m) [16].

	Air Temperature (℃)	Relative humidity	Daily solar radiation horizontal (kWh/m^2/day)	Heating degree-days (℃-Days)	Cooling degree-days (℃-Days)
January	−1.6	64.3%	2.82	608	0
February	0.5	61.0%	3.69	490	0
March	5.7	59.7%	4.49	381	0
April	12.5	59.4%	5.40	165	75
May	17.7	66.9%	5.57	9	239
June	22.0	72.8%	4.99	0	360
July	25.1	80.2%	4.17	0	468
August	25.5	79.5%	4.19	0	481
September	20.5	77.1%	3.95	0	315
October	13.9	73.2%	3.55	127	121
November	7.2	71.0%	2.76	324	0
December	0.9	67.9%	2.55	530	0
Annual	12.6	69.5%	4.01	2,634	2,058

Higher building thermal capacity indicate higher potential for reducing energy consumption during the on-peak period by shifting more thermal load. The building tested in this study is a demonstration house for a low-energy solar house. To reduce thermal demand considerably, the thickness of the thermal insulation was approximately twice that of the thermal insulation of the conventional houses in Korea. The thickness of the insulation used for the roof, external walls, and floors is approximately 250 mm. The walls of the house were constructed using concrete. The characteristics of the material used for constructing buildings affect their thermal capacity or thermal inertia. The thermal time constant can be expressed as a product of thermal resistance and thermal capacitance, which is one of the most important characteristic parameters of buildings. The building tested in this study has approximately twice the insulation thickness than that of conventional houses in Korea. Thus, the thermal time constant of the house would be approximately twice that of the conventional houses. However, a more detailed evaluation is required to analyze the impact of building materials by using a calibrated building simulation model as a future study.

5. Conclusions

In this study, simple strategies for thermal storage control were proposed for space-cooling and space-heating operation modes. The objective of the control strategies is to minimize the electricity consumption for space cooling and space heating during the peak period. The duration of the peak period in this study was assumed to be 3 h, from 2 pm to 5 pm, for space cooling, and 3 h, from 5 pm to 8 pm, for space heating. The control strategies applied in this study adjust the setpoint temperatures for the heat pump and the indoor space to utilize buffer thermal storage and building thermal mass to shift thermal demand during the on-peak period to the time period prior to the on-peak period in space cooling mode. On a peak day in winter, a similar control strategy that uses buffer thermal storage and building thermal mass were employed. In this study, the additional thermal storage of a solar hot water storage

tank is involved. To evaluate the potentials of control strategies using the thermal storage of the building thermal mass and a thermal storage tank, experimental tests were performed at a demonstration solar house. The control strategies showed good performance when reducing the energy consumption during the peak period. In particular, CSC exhibited zero energy consumption for both space cooling and space heating during the peak period. For the space-cooling test, it is noted that negative net electricity consumption was possible, provided that electricity generation from the solar PV system was utilized throughout the peak period. BSC also showed similar performance, with negative net energy consumption because of solar PV electricity generation. For the space heating mode tests, the impact of the solar PV system was negligible because the on-peak period was assumed to occur in the late afternoon and evening, between 5 pm to 8 pm.

In this study, the aim of the control strategy is to shift the energy demand away from the peak period by employing a constant indoor setpoint temperature during the peak period. However, if the objective of the control strategy is to make the net electricity demand negative throughout the peak period, then the setpoint should be adjusted in a non-linear trajectory so that the electricity consumption for the space-cooling system is reduced from the start to the end of the peak period (because the output of the solar PV generation decreases during this period). To obtain the trajectory of the setpoint, an approach based on the optimization of either the physical building model or a data-driven model must be developed. Further studies are necessary to evaluate the impact of different control parameters such as setpoint temperatures and their duration. The duration of the peak period is another important parameter to consider. For example, peak power demand can occur sometime between 10 am to 12 pm and 2 pm to 5 pm on the Korean National Grid. More comprehensive studies can be performed using a detailed building system simulation model that has been calibrated with the measured data. A generic control strategy that can obtain a site-specific control strategy from basic principles and methodologies should also be developed.

Acknowledgments

This work was conducted under the framework of Research and Development Program of the Korea Institute of Energy Research (KIER) (B5-2509).

Author Contributions

Kyoung-ho Lee designed the experiments and analyzed the performance of the storage control strategies for the experimental study, Moon-chang Joo performed experiments, and Nam-choon Baek analyzed the operation of the system.

Conflicts of Interest

The authors declare no conflict of interest.

References

1. Sun, Y.; Wang, S.; Xiao, F.; Gao, D. Peak load shifting control using different cold thermal energy storage facilities in commercial buildings: A review. *Energy Convers. Manag.* **2013**, *71*, 101–114.

2. Ban, M.; Krajacic, G.; Grozdek, M.; Curko, T.; Duic, N. The role of cool thermal energy storage in the integration of renewable energy resources and peak load reduction. *Energy* **2012**, *42*, 298–304.
3. Henze, G.P.; Felsmann, C.; Knabe, G. Evaluation of optimal control for active and passive building thermal storage. *Int. J. Therm. Sci.* **2004**, *43*, 173–183.
4. Liu, S.; Henze, G.P. Experimental analysis of simulated reinforcement learning control for active and passive building thermal storage inventory: Part 1. Theoretical foundation. *Energy Build.* **2006**, *38*, 142–147.
5. Liu, S.; Henze, G.P. Experimental analysis of simulated reinforcement learning control for active and passive building thermal storage inventory: Part 2. Results and analysis. *Energy Build.* **2006**, *38*, 148–161.
6. Hajiah, A.; Krati, M. Optimal controls of building storage systems using both ice storage and thermal mass—Part I: Simulation environment. *Energy Convers. Manag.* **2012**, *64*, 499–508.
7. Hajiah, A.; Krati, M. Optimal controls of building storage systems using both ice storage and thermal mass—Part II: Parametric analysis. *Energy Convers. Mananag.* **2012**, *64*, 509–515.
8. Barzin, R.; Chen, J.; Young, B.R.; Farid, M.M. Peak load shifting with energy storage and price-based control system. *Energy* **2015**, in press.
9. Lee, K.H.; Braun, J.E. Model-based demand-limiting control of building thermal mass. *Build. Environ.* **2008**, *43*, 1633–1646.
10. Lee, K.H.; Braun, J.E. Development of methods for determining demand-limiting setpoint trajectories in buildings using short-term measurements. *Build. Environ.* **2008**, *43*, 1755–1768.
11. Lee, K.H.; Braun, J.E. Evaluation of methods for determining demand-limiting setpoint trajectories in buildings using short-term measurements. *Build. Environ.* **2008**, *43*, 1769–1783.
12. Lee, K.H.; Lee, J.-K.; Yoon, E.-S.; Joo, M.-C.; Lee, S.-M.; Baek, N.-C. Annual measured performance of building-integrated solar energy systems in demonstration low-energy solar house. *J. Renew. Sustain. Energy* **2014**, *6*, 042013.
13. NatHERS—Nationwide House Energy Rating Scheme. Available online: http://nathers.gov.au/about/heatloads.php (accessed on 14 August 2013).
14. Korea Electric Power Corporation (KEPCO) Research Institute. *Development of Standardized Model of Fully-Electrified House*; Technical Report TR.1324.S2013.0001; KEPCO: Daejeon, Korea, 31 October 2012; pp. 40–45, 151–153.
15. KPX, Korea Power Exchange. Available online: http://power.kpx.or.kr/english/ (accessed on 1 June 2015).
16. RETScreen Tools, Climate Data Provided by NASA. Available online: http://www.retscreen.net (accessed on 17 August 2015).